Soft Matter

Speedy one-pot electrochemical synthesis of giant octahedrons from in situ generated pyrrolidinyl PAMAM dendrimer

Journal:	*Soft Matter*
Manuscript ID	SM-ART-05-2020-000819.R1
Article Type:	Paper
Date Submitted by the Author:	19-Jun-2020
Complete List of Authors:	Singhania, Anup; CSIR-North East Institute of Science and Technology, Chemical Science and Technology Division; Academy of Scientific and Innovative Research Dutta, Mrinal ; CSIR-National Physical Laboratory Advanced Materials and Device Metrology Division, PV Metrology Section, Division of Advanced Materials, Devices and Metrology Saha, Supriya; Visva-Bharati, Chemistry Sahoo, Pathik; Sun Yat-Sen University, depathment of Chemistry and Chemical Science Bora, Bharati; North East Institute of Science and Technology CSIR Ghosh, Subrata; CSIR-North East Institute of Science and Technology, Chemical Science and Technology Division; CSIR North East Institute of Science & Technology Fujita, Daisuke; National Institute for Materials Science, Bandyopadhyay, Anirban; Advanced Nano Characterisation Center (ANCC), Advanced Scanning Probe Microscopy group

ARTICLE

Speedy one-pot electrochemical synthesis of giant octahedrons from *in situ* generated pyrrolidinyl PAMAM dendrimer

Received 00th January 20xx,
Accepted 00th January 20xx

DOI: 10.1039/x0xx00000x

Anup Singhania,[a,e] Mrinal Dutta,[b,f] Supriya Saha,[c,e] Pathik Sahoo,[d] Bharati Botra,[a] Subrata Ghosh*,[a,e] Daisuke Fujita[d], Anirban Bandyopadhyay[d]

A novel electrochemical synthesis via a radical generation pathway is described here for the generation of quaternary megamer structure from secondary dendrimers. The reaction is rapid and completes in <5 min. We have used lower/higher generation poly(amido)amine (PAMAM) dendrimers with carboxylic acid groups at the terminals. A precise electrocatalytic reaction at >3.5V activates the carboxylic groups to undergo anodic oxidation (-e$^-$) and produce radical carboxylate anions on the dendrimer surface. The reaction further goes through a decarboxylative elimination. Successive self-assembly creates billions of polydispersed and extremely stable ~500nm octahedron nanostructures, which we failed to destroy even by using a 20kV electron beam. This is a new route for the speedy synthesis of important futuristic material of well-defined shape. It has applications in building designer organic crystals for solar cells, organic electronics, rapid protein gelation, and rapid protein crystallization, etc.

Introduction

Dendrimers have unique secondary structures, which are good building blocks for the rapid construction of large nanostructures with higher complexity.[1,2] Intermolecular covalent bonding of dendrimers produce megamer, some of them form a linear chain, and some of them resemble crystals.[3,4] Nanocomposite and nanoparticle synthesis follow the dynamics of self-assembly.[5,6] However, oligomerization is commonly observed in biological systems. Many complex molecular structures self-assemble into oligomers of different shapes. For example, the primary structure of proteins (polypeptide chains) can naturally form secondary helical/beta-sheet structures that self-assembles into tertiary and quaternary megamers or superstructures. Such self-assembled protein-megamers are the initiators and responsible for many protein-related life-threatening diseases.[7,8] Therefore, artificial protein-mimicked structures are the popular substrates for initiating characteristic changes in the key protein secondary structures underpinning the corresponding influencing factors. We preferably selected dendrimers (starburst polymers) well known for their unique polymeric structures having a sphere-like shape with branches spreading outwardly from a single core. The ideal spherical shape of the dendrimers allows their uniform distribution of functional groups and charges on their surface.[9] Poly(amido)amine (PAMAM) dendrimers are the most appropriate candidates among the protein-mimic artificial polymers because the biocompatibility of PAMAM dendrimers may be modulated via molecular engineering[10] and the polyamide chains can form the secondary starburst structure.[11] Therefore, inter-branch electronic and hydrogen bonding interactions between the closely spaced amide groups from different dendrites of the dendrimer is strong and highly sensitive to some external factors like pH, electrostatic field, heat, etc. The PAMAM dendrimers, therefore, possess a sphere-like regular shape when suspended in solution and even during the solid-state support.[12,13]

With the incremental fractal growth in the branch chains, the size of

[a] *Chemical Science & Technology Division, CSIR-North East Institute of Science & Technology, Jorhat, Assam-785006, India. E-mail: ocsgin@gmail.com*
[b] *PV Metrology Group, Advanced Materials Devices and Metrology Division, CSIR-National Physical Laboratory, New Delhi-110012, India*
[c] *Advanced Computation and Data Sciences Division, CSIR-North East Institute of Science & Technology, Jorhat, Assam-785006, India.*
[d] *International Center for Materials and Nanoarchitectronics (MANA) and Research Center for Advanced Measurement and Characterization (RCAMC), National Institute for Materials Science (NIMS), 1-2-1 Sengen, Tsukuba, Japan*
[e] *Academy of Scientific and Innovative Research (AcSIR), CSIR-NEIST Campus, Jorhat, Assam 785006, India*
[f] *Academy of Scientific and Innovative Research (AcSIR), CSIR-NPL Campus, New Delhi-110012, India*
† Footnotes relating to the title and/or authors should appear here.
Electronic Supplementary Information (ESI) available here. See DOI: 10.1039/x0xx00000x

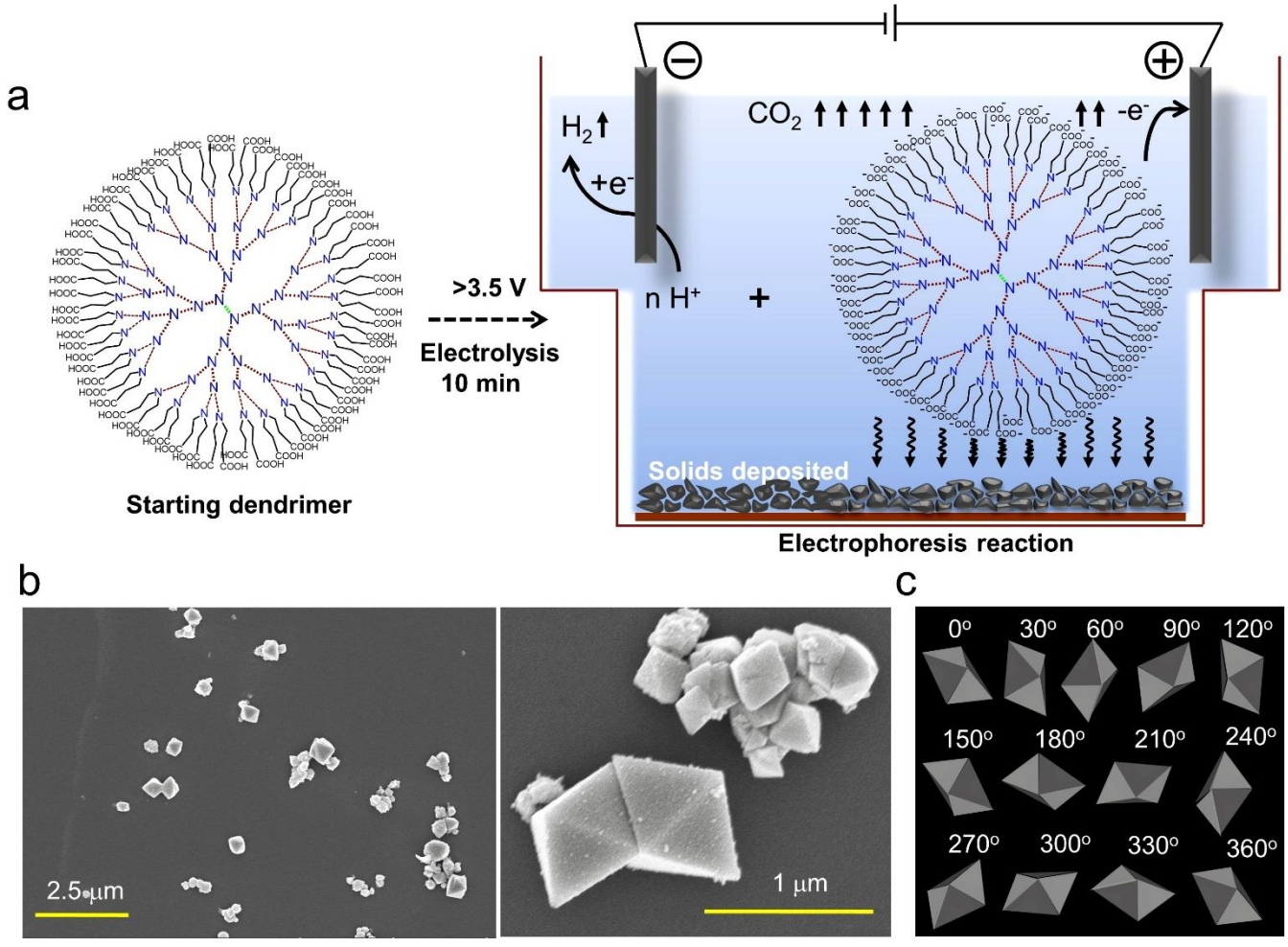

Figure 1. (a) Schematic representation of self-assembly of PAMAM EDA core/COOH terminals dendrimer under electrolysis condition (applied voltage between the electrodes is 3.5 V and more as required, applied for 10 min). (b) SEM images of octahedron architecture from above self-assembly of PAMAM dendrimer. (c) top view of octahedron crystal from different angles.

a starburst polymer increases, and therefore, it also changes the intrinsic vibrational dynamic fluctuation.[14,15] We know that depending on the chemical structure, the dynamical property of the molecular branches could be tuned.[16] As the generation of iterative function increases, the degree of dynamic behavior increases significantly in a dendrimer, which is a deterministic factor for self-assembly to form the megamer nano-structure of a defined shape. One of the most featured examples is the formation of quaternary core-shell tecto-dendrimer structure by the two or more different generations of dendrimers via self-assembly or covalent bonding between the complementary surface functionalities.[17] Again, the shape of the megamer architecture resulted from the self-assembly of a particular dendrimer type is very much dependent on the generation of the dendritic branches. Under certain experimental conditions, the formation of quaternary megamer (core-shell tecto-dendrimer) from PAMAM dendrimers requires end-terminal functionalization.[18,19] Two kinds of PAMAM dendrimer terminals undergo a megamer formation.[20] One type of dendrimer could have a large number of -NH_2 terminals, and the other, smaller dendrimers, might have complementary ester termini. However, sometimes such assemblies of the dendrimers produce ill-defined megamer structures via an anisotropic growth by chemical bonding. In a few cases, isotropic growth is also observed.[21,22]

There are many experimental shreds of evidence for the differential growth features of the starburst polymers.[23-25] It is also observed that dendrimers act as potential moieties in liquid crystals. Therein,

the dendrimers flip between two opposite tendencies. Inhomogeneous

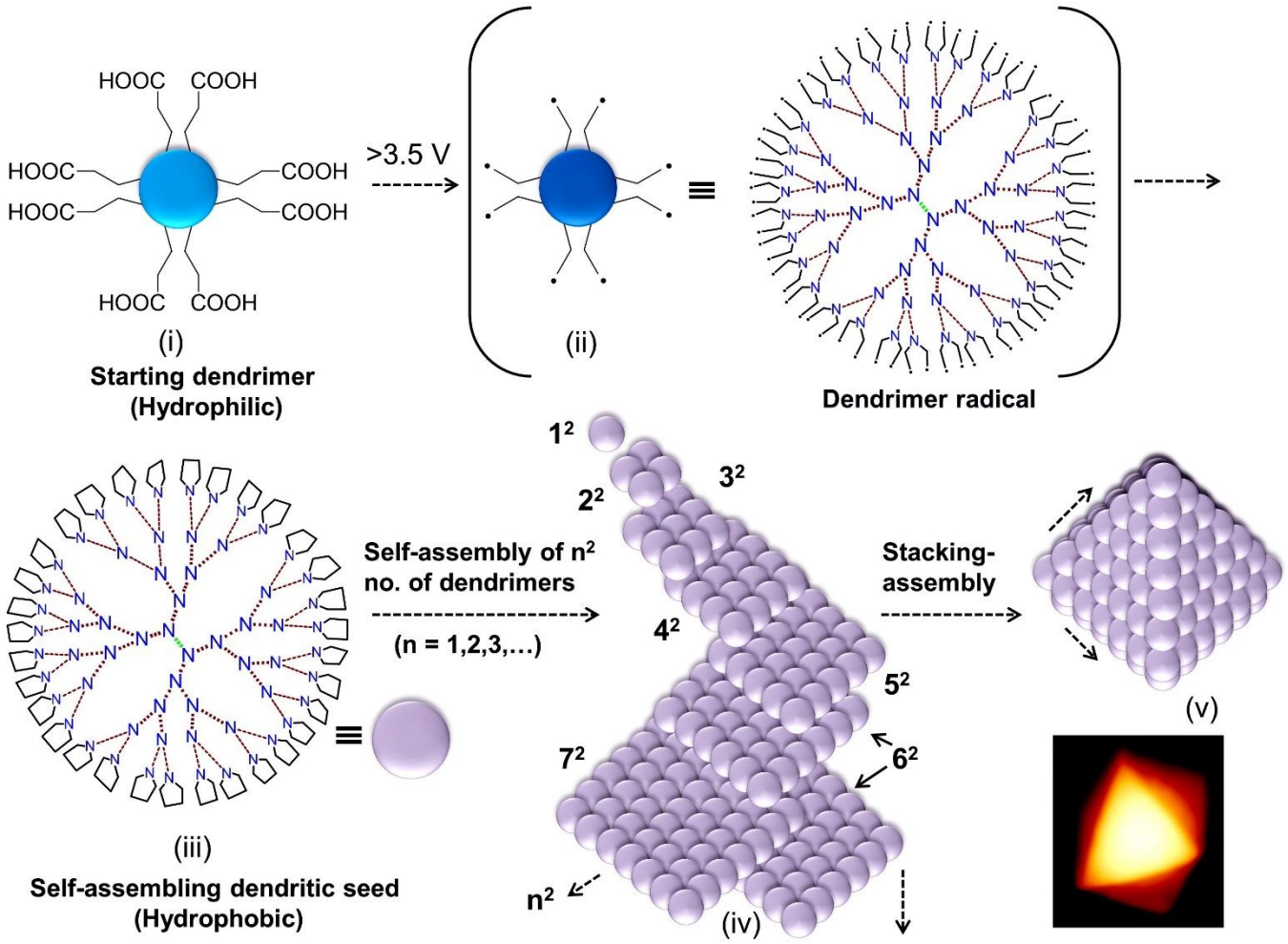

Figure 2. Schematic representation for the preparation of heterocyclic pyrrolyl dendrimer via a radical mechanism. Further stacking of the hydrophobic dendritic seed via self-assembly building an octahedron architecture.

distribution leads to an anisotropy of the structural unit and the isotropic dendritic framework. PAMAM dendrimer forms liquid crystals following a simple modification of the terminal functional groups.[26] Here, we modify the terminals of PAMAM dendrimers so that different electrocatalytic processes are initiated for the synthesis of supramolecular assembly. Consequently, we have used these various embedded properties of the starburst PAMAM dendrimer structures.

Materials and methods

All the PAMAM dendrimers, i.e., G3.5 dendrimer with ethylene diamine core/COOH terminals [$[NH_2(CH_2)_2NH_2]$:(G=3.5); dendritic $PAMAM(NHCH_2CH_2COONa)_{64}$], G5.5 dendrimers with ethylene diamine core/COOH terminals [$[NH_2(CH_2)_2NH_2]$:(G=5.5); dendritic $PAMAM(NHCH_2CH_2COONa)_{256}$] were purchased from Aldrich Chemicals and purity of all samples are crosschecked by analytical characterizations. De-ionized Milli-Q water (18 MΩ) was obtained from a Millipore purifier. Soldering wire (Sn: Pb) used for electrolysis was purchased from commercial sources. A dc power source is used to supply the required voltage (>3.5V) between the electrodes, regulating the current flow less than a 1 microampere.

The general procedure of sample preparation for the electrolysis reaction of PAMAM dendrimer generation 3.5 & 5.5

In a pear-shaped flask, the methanol solution of the PAMAM G3.5 dendrimer is taken, and then methanol is removed under vacuum. Then Milli-Q water is added to re-solubilize the solid film. Then we added (1:1) formic acid solution and stirred it at room temperature for 5 h. Then the reaction mixture is dialyzed for overnight following cellulose membrane dialysis tubing method in the Milli-Q water medium. Dialysis helps to remove the organic salt (sodium formate), which is a by-product of the reaction. Thus, all the -COONa end groups of the dendrimer surface are acidified to the required -COOH functional groups (Figure S1 shows the scheme of acidification). Similarly, G5.5 dendrimer is also acidified. Thus, carboxylic acid functional group-containing dendrimer samples are prepared for the electrocatalysis reaction.

The general procedure of electrocatalysis reaction of PAMAM dendrimer generation 3.5 & 5.5 contain -COOH terminal groups

We have used a various micromolar aqueous solution of PAMAM(-COOH-terminals dendrimers of different generations and sent dc voltage (3.5-5.0 V) through the solutions in a 1x1 cm diameter cuvette. The reaction is continued until effervescence from the solution is ceased. The white-colored solid particle deposition at the bottom of the reaction chamber was a very slow process. The cloudy solution took more than half an hour to precipitate as white particles.

Structure characterization by Field Emission Scanning Electron Microscopy (FESEM)

Aqueous solutions of the samples were prepared and drop cast on the carbon tapes and the clean glass substrates. These coated carbon tapes and glass substrates were vacuum dried. After complete drying, these samples were taken for SEM observations (Carl ZEISS Microscopy, Germany). From the SEM images, the size variation statistics for three distinct synthesis outcomes are summarized in the histogram plotted in Figure S6.

During the SEM experiment, we sent an intense electron beam (20 kV) in the samples, but any degradation of the nanostructures was not found. Thus, assembled supramolecular structures exhibit extreme stability under the high energy electron beam in SEM.

Structure characterization by FTIR spectroscopy

We have analysed the FTIR (model: Perkin-Elmer, model: Spectrum 100) of the megamers formed in the reaction. Since we did not find any evidence of strong covalent bonding via FTIR, the architecture forms possibly only via physical bonding.

Structure characterization by High Resolution Transmission Electron Microscope (HRTEM)

The aqueous solution of the compound was drop cast on the surface of the copper grid (carbon film copper mesh 400). The TEM image (JEOL, Japan; model: JEM-2100 PlusElectron Mocroscope) of the sample shows a regular surface characteristic.

Structure characterization by X - ray powder diffraction (XRPD)

X – ray powder diffraction (XRPD) analysis was carried out to determine the crystal structure of the megamer resulted from PAMAM G3.5 and G5.5 dendrimers using a Rigaku X – ray diffractometer, model: ULTIMA IV, Rigaku, Japan.

Structure characterization by X-ray Photoelectron Spectroscopy (XPS)

XPS study (Thermo Fisher Scientific Pvt. Ltd., UK, model: ESCALAB Xi+) shows that metals are released in the solution during the electrolysis process due to leaching of the electrode surface. Therefore, any positive role of the metal ions in creating the octahedron shape is not confirmed.

Theoretical simulation study

After basic molecular mechanics (semi-empirical) studies to understand various processes and mechanisms, we carried out theoretical calculations using the density functional theory (DFT) with the Gaussian 16 (G16) suite of programs[27]. The structure of the reactants, intermediates, and products was optimized at the B3LYP level of theory using the 6-31G(d) basis set.

Results and Discussion

There are two ways the self-organization: by segregation of incompatible molecular subunits into the molecular subspace accompanied by the aggregation of compatible molecular subunits. Second, the minimization of free volume to allow a parallel alignment of the anisometric molecular subunits.[28-30] In the current

report, we will discuss the electrochemical surface-modification and self-assembly of the PAMAM dendrimers into the regular octahedrons of various sizes. From the experiments of PAMAM G3.5 and G5.5 dendrimers, we propose that during an electrolytic process,[31-33] an equivalent single electron transfer process on the anode results in the formation of radical carboxylate ions on the dendrimer surface. Then from the bulk of the solution, the decarboxylation reaction takes place, as shown in Figure 1. Subsequently resulted in poly-radical dendrimer species end up forming a heterocyclic five-membered ring structure at the surface of the dendrimer molecules. In the next step, the hydrophobic nature of the dendrimer surface due to the pyrrolidine groups triggers the supramolecular assembly (Figure 2). Figure S6 shows a histogram of the octahedron formation. It suggests a quantized jump in size distribution, with a peak at 486nm ±12nm (SD). However, some irregular megamer architectures are also produced in the same reaction solution. We could observe a generic trend of self-assembly to produce a definite octahedron irrespective of the size of a single dendrimer structure. We describe two generations of dendrimers here. The two cases are: the first megamer is formed by PAMAM dendrimers of G3.5 dendrimer with ethylene diamine core/COOH terminals $[[NH_2(CH_2)_2NH_2]$:(G=3.5);dendritic PAMAM$(NHCH_2CH_2COONa)_{64}]$, and the second megamer is formed by G5.5 dendrimers with ethylene diamine core/COOH terminals $[[NH_2(CH_2)_2NH_2]$:(G=5.5); dendritic PAMAM$(NHCH_2CH_2COONa)_{256}]$. We could explore the probable chemistry of the stacking-assembly pattern of carboxylic acid terminal PAMAM dendrimers. We discuss the process of electrolysis of -COOH terminal PAMAM dendrimer varieties in solution in Milli-Q water. Here during the electrochemical process, we have prepared the cathode and anode by soldering wire (Sn). Two electrodes are kept at two ends of the electrolysis chamber (roughly a 1 cm separation is maintained between the two electrodes). However, spacing does not affect an electrochemical process. It is not a field-induced phenomenon. When bias drives synthesis, the product is fixed, irrespective of the distance between the electrodes. Here the only electrolyte is a PAMAM dendrimer with carboxylic acid terminals; it has high critical potential. So at the cathode surface, Sn (E^0_{red} is higher than H^+) may initiate the ionization of the carboxylic acids to carboxylate ions. PAMAM dendrimer forms a salt, which is the primary requirement for Kolbe's electrolysis. The possible reactions are as follows:

$Sn \rightarrow Sn^{2+} + 2e^-$

$2H^+ + 2e^- \rightarrow H_2\uparrow$

Here Pt-electrode cannot initiate such ionization. A decarboxylation reaction is only possible if a particular type of electrode is used;[34] therefore, our observation is in line with earlier findings. Kolbe's reaction is carried out by gold, palladium, platinum, and gold-palladium alloys electrodes, only for small molecules.[35] If there is a large molecule, electrode specificity becomes prominent. During the electrolysis process, we observed gas emission (H_2) from the cathode, whereas bubbles of emission were also observed quite away from the electrodes, from the bulk of the electrolyte solution. Therefore, from the structural precondition of the molecules & the solvents, we assumed that the two gases were hydrogen and carbon dioxide gases produced respectively due course of the electrolysis, which were further confirmed chemically. Effervescence in the cathode is due to the liberation of hydrogen gas by the carboxylic acid groups. The effervescence from the bulk of the solution is due to the liberation of carbon dioxide gas by the carboxylate radical ions on the dendrimer surface. Separately, if Sn^{2+} is added to the dendrimer solution alone, no reaction happens.

To analyze the feasibility and stability of the final products, observed experimentally in the electrolysis process, releasing of H_2 gas from the cathode, and CO_2 gas away from electrodes, i.e., from the bulk of the electrolyte solution. The presence of CO_2 was confirmed by passing the gas through diluted calcium hydroxide. Furthermore, using molecular mechanics and semiempirical studies, we have performed theoretical calculations on the formation of supramolecular assemblies. We considered the most probable reaction mechanism presented in scheme 1. In FTIR analysis distinguished peaks for N-H, C=O, C-H, and other fingerprint regions have appeared. Therefore, structures are doubtlessly generated from the PAMAM molecules.

The possibility of forming the scale-free polydispersed octahedrons via self-assembly depends on the non-covalent assembly of closely spaced PAMAM units. The synthesis results in '(n x n) [n (integer number) = 1,2,3,...any integer]' the 2D nano-sheets of various layers. The increment of participating dendrimer molecule in stacked-layer followed the rule of numbers with the variation of n^2. These 2D nano-sheets could thereby self-assemble in a 3D

structural over-growth of the regular geometric shape varying from a few nm to a few mm in diameter (Figure 1). The observation can be explained via the two-step process. In the first step, a dendrimer poly-alkyl radical intermediate species forms via decarboxylation of the carboxylic acid radical ions (Gibbs free energy for this reaction is -107.95 Kcal/mol) at the dendrimer terminals. In the second step, a stable hydrophobic pyrrolidine ring is formed. The Gibbs free energy for the formation of pyrrolidine ring from alkane radical is -8.42 Kcal/mol. We simplified the theoretical structure to study the mechanism of the site-based reaction within reasonable computational time and cost. Instead of the whole dendrimer, a single linear branch of the dendrimer was considered to represent the homogeneous distribution of reaction mechanism centers. It is mimicking the formation of oligomer like structure from the dendrimers (Scheme 1).

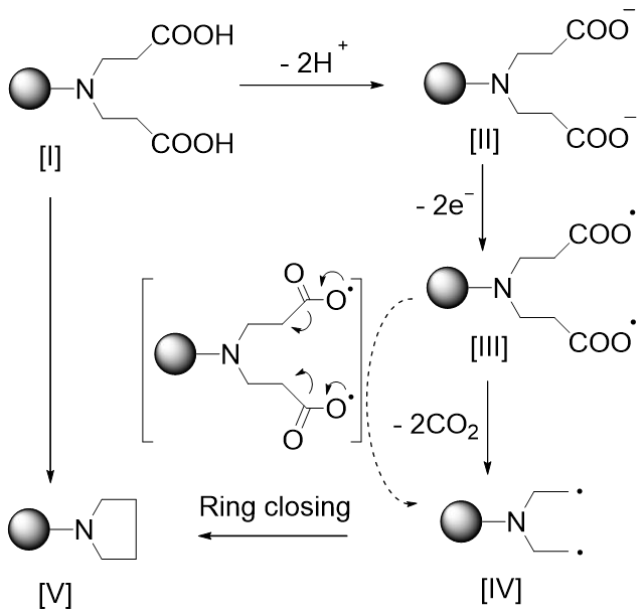

Scheme 1. A plausible mechanism for the formation of a stable hydrophobic pyrrolidine ring in the corresponding PAMAM dendrimer's terminal end.

However, at the same time, many of the activated COOH-terminal dendrimers could not self-assemble into a regular shape. Several radical species do not participate in forming the pyrrolidine ring. They rather compete with a terminal alkane chain formation that inhibits building any periodic assembly.[36,37] It might have led to the morphologically irregular structures.

Since we used soldering wire (Sn: Pb) as the electrodes, therefore, we were extremely concerned about the incorporation of metal ions during self-assembly. To clear our doubts about the metal ion release from the cathode to the solution, we repeatedly checked the solution's electrochemistry even during the chemical reaction. The theoretical finding also confirmed the experimental analysis of the product under the X-ray photoelectron spectroscopy (XPS). In the qualitative XPS analysis, we have compared two solutions, one sample, and the other one was a blank solution. The first XPS sample was prepared by carrying out electrolysis on pure water without any dendrimer. The second sample was prepared, post electrolysis of the dendrimer solution. Our observations show the presence of metals, e.g., tin (Sn), zinc, and lead (Pb) in both the solutions whose origin is the electrodes used for the electrochemical process. Trace of tin (Sn) and lead (Pb) remains constant in the solution irrespective of the duration of synthesis. We estimated the Sn: Pb amount for various durations and found that at the beginning of synthesis, the electrodes release Sn and Pb, and the electrodes turn black. Afterward, an equilibrium is reached, then, Sn and Pb are not released in the solution. The electrocatalysis of PAMAM continues at the Sn: Pb electrode. However, the participation of any specific metal/ion in the octahedron architecture formation is not established even after rigorous EDX studies. Thus, we confirm, the metallic ions are not part of the octahedron crystals irrespective of varying sizes.

Spectroscopic studies to understand the inner structures of giant octahedron.

The Infrared (IR) spectroscopy was carried out on PAMAM G3.5, PAMAM G3.5 megamers, PAMAM G5.5, and PAMAM G5.5 megamers to confirm the molecular structure. The carboxylic groups in PAMAM exhibit a unique feature, where the standard carboxylic stretching frequencies never appear around 1700cm^{-1}.[38] Such carboxylic acid groups can only be confirmed after esterification, where the strong carbonyl stretching frequency appears at 1735cm^{-1}.[39] These carboxylic groups can form zwitterion with the neighbor amines and appear as carboxylate in the solid-state structure.[40,41] In zwitterion, the proton from carboxylic acid is transferred to the amine group and forms the carboxylate salt. An IR spectrum of PAMAM G3.5 exhibits two broad peaks at 1634cm^{-1}, and 1569cm^{-1} can be attributed to amide I and amide II stretching frequencies. Interestingly, the presence of an ammonium group for zwitterion makes the higher energy region (~3700-2800 cm^{-1})

broader along with CON-H stretching frequency. Carboxylate peaks (COO-) cannot be distinguished here as it merges with the amide peaks. At 1404cm-1, O-H bending is appearing. Two close peaks at 1132cm^{-1} are attributed to the asymmetric 1143cm^{-1} and symmetric 1132cm^{-1} stretching frequencies arising from imidic acids, formed in amide driven tautomeric process.

In the FTIR of PAMAM G3.5 monomer, the carboxylate peaks merge with that of the amides. When monomers bind into the megamers of PAMAM G3.5 by decarboxylation, in the product, there is no visible sign of the COO- peaks. However, when G3.5 monomer forms a megamer, 5-member ring forms at the external surface of PAMAM, one can assign the stretching of the C-N bond at 1188cm^{-1}. Generally, this C-N bond does not always appear in the IR spectroscopy. In the decarboxylation process, the monomer loses the ammonium ion as it converts to tertiary amine while forming the megamer. As a result, the broadness of the peak at the higher energy region of a monomer decreases as it forms the megamer. In PAMAM megamers, along with the two amide peaks (1632, 1590 cm^{-1}), a small peak at 1655 cm^{-1} appeared for N-H stretching mode.

After electrolysis, PAMAM G5.5 self-assembles to form PAMAM G5.5 octahedron megamers and shows peaks at 1603cm^{-1} (stretching, HN-C=O), and 1388cm^{-1} (O-H bending). As we shift from G3.5 to G5.5 version, the PAMAM G5.5 FTIR spectrum similarly shows the peaks at 1631cm^{-1} (strong, HN-C=O stretch), 1572cm^{-1} (strong, HN-C=O stretch), and 1399cm^{-1} (medium, O-H bend). Similar to G3.5, when the monomer of G5.5 converts to the megamer of G5.5, then, the broadness of the peak at the higher energy region decreases, but not as significantly as G3.5. Due to the increment of generations, the CN stretching and tertiary amine peaks as nearly masked. However, the CON-H stretching (3421cm^{-1} strong,) and N=C-O-H stretching (3290cm^{-1}, medium) are still explicit in the megamer.

X– ray powder diffraction (XRPD) analysis was carried out to determine the crystal structure of the G3.5 and G5.5 using a Rigaku X – ray diffractometer (model: ULTIMA IV, Rigaku, Japan). XRPD instrument was operated with a scanning rate of 3^{o} min^{-1} in the 2θ value ranging from 2–75^{o} with a CuKα X – ray radiation (λ = 1.54056 Å). In case of G3.5, the diameter of molecule is 4 nm, which should correspond to the peak at 2.2°. Whereas, diffraction at 1.45° can be expected for G5.5 as it has the 6nm molecular diameter. Both the compounds diffract poorly and exhibit two broad peaks around 12° and 24.5°. We cannot determine the exact d-spacing between two planes. The average distance, d ~ 0.74 nm (corresponds to 12°) and d~0.36 nm (corresponds to 24.5°) came from intramolecular packing pattern, which would require further investigation.

Spectroscopic studies FTIR and XRD suggest that the extremely solid octahedrons are organic solid, they are made of dendrimers only, however, ordering is limited to 4-5nm only, the geometric arrangements of the superclusters currently appears not possible, investigations are on to slow down rapid reaction rate so that long range ordered crystals could be formed.

Conclusions

PAMAM dendrimers are unstable, degrade naturally. However, when electrochemical synthesis binds them into octahedron superstructures, it becomes very stable. They do not destroy even under an intense 20kV electron beam. Higher generation PAMAM structures have similarities to the peptide structures, so the Sn-electrode based electrocatalysis may be used for precipitating proteins as a crystal for a better structural analysis. The fractional presence of metallic impurity catalyzes superstructures of various kinds. If it was simply base/Sn^{2+} catalysis, then the reaction could not terminate within 5 minutes of bias applied, and we would have observed that. We have made an effort to understand and investigate how fractal branches of dendrimers could be used to trigger rapid crystallization. It would help to replicate the aggregation of proteins, in vitro, a key to many diseases. For example, neurodegeneration leads to the fatal segregation of neurofibrils. Such structures could be recreated in vitro to learn Alzheimer's.

Conflicts of interest

There are no conflicts of interest.

Acknowledgments

Authors acknowledge SERB, Govt. of India for research grant [no. ECR/2016/001534(2017-2020)], CSIR, India for research grant [no. HCP-021(2019-2020)], the JSPS Grants in Aid for Young Scientists (A) for 2009-2011, Grant number 21681015 (Govt of Japan), and Asian office of Aerospace R&D (AOARD) a part of United States Air Force (USAF) for the Grant no. FA2386-16-1-0003 (2016–2019). Authors thank CSIR-NEIST &

NIMS Sengen site for providing infrastructure support and analytical facilities; also acknowledge the Academy of Scientific and Innovative Research (AcSIR), India. Authors also acknowledge Dr. Binoy K Saikia, Dr. Prasenjit Saikia and Dr. Biswajit Saha for analytical supports.

References

1. D. A. Tomalia, A. M. Naylor and W. A. Goddard, *Angew. Chem. Int. Ed. Engl*., 1990, **29**, 138-175.
2. M. A. van Dongen, S. Vaidyanathan and M. M. Banaszak Holl. *Soft Matter*, 2013, **9**, 11188-11196.
3. J. Barberá, B. Donnio, L. Gehringer, D. Guillon, M. Marcos, A. Omenat and J. L. Serrano. *J. Mater. Chem.*, 2005, **15**, 4093-4105.
4. S. C. Zimmerman, F. W. Zeng and D. E. C. Reichert, *Science*, 1996, **271**, 1095–1098.
5. G. P. Baeza, C. Dessi, S. Costanzo, D. Zhao, S. Gong, A. Alegria R. H. Colby, M. Rubinstein, D. Vlassopoulos, and S. K. Kumar, *Nat. Commun.*, 2016, **7**, 11368.
6. N. Jouault, D. Lee, D. Zhao and S. K. Kumar, *Adv. Mater.* 2014, **26**, 4031–4036.
7. C. M. Dobson, *Nature,* 2002, **418**, 729–730.
8. M. Vendruscolo, J. Zurdo, C. E. MacPhee and C. M. Dobson, *Phil. Trans. R. Soc. Lond. A*, 2003 **361**, 1205–1222.
9. P. K. Maiti, T. Çağın, G. Wang, William A. Goddard, *Macromolecules,* 2004, **37**, 6236-6254.
10. S. Ghosh, A. Roy, A. Singhania, S. Chatterjee, S. Swarnakar, D. Fujita and A. Bandyopadhyaya, *Toxicology Reports*, 2018, **5**, 1044-1052.
11. D. A. Tomalia, *Soft Matter*, 2010, **6**, 456-474.
12. G. M. Whitesides and B. Grzybowski, *Science*, 2002, **295**, 2418-2421.
13. P. Carbone and F. M. Plathe, *Soft Matter*, 2009, **5**, 2638–2647.
14. H. J. Kim, T. Kim, M. Lee, *Acc. Chem. Res*., 2011, **44**, 72−82.
15. S. Ghosh, M. Dutta, S. Sahu, D. Fujita and Anirban Bandyopadhyay, *Adv. Funct. Mater.*, 2013, **24**, 1364-1371.
16. E. Rodrigo, H. Baunis, E. Suna, and S. R. Waldvogel, *Chem. Commun.*, 2019, **55**, 12255–12258.
17. T. Xiao, W. Zhong, L. Xu, X. Q. Sun, X. Y. Hu and L. Wang *Org. Biomol. Chem*., 2019, **17**, 1336-1350.
18. K. Sajjad, D. Mitra, M. Hamid and A. I. Sepideh, *Soft Matter*, 2018, **14**, 3151-3163.
19. S. Ghosh, S. Chatterjee, A. Roy, K. Ray, S. Swarnakar, D. Fujita and A. Bandyopadhyay, *Curr. Top. Med. Chem.*, 2015, **15**, 534-541.
20. J. M. J. Frechet, *PNAS*, 2002, **99**, 4782-4787.
21. D. A. Tomalia, H. M. Brothers, L. T. Piehler, H. Dupont Durst and D. R. Swanson, *PNAS*, 2002, **99**, 5081–5087.
22. F. Chen, L. Kong, L. Wang, Y. Fan, M. Shen and X. Shi, *J. Mater. Chem.* B, 2017, **5**, 8459.
23. H. Wang, W. Miao, F. Wang and Y. Cheng, *Biomacromolecules,* 2018, **19**, 2194−2201.
24. T. Wei, C. Chen, J. Liu, C. Liu, P. Posocco, X. Liu, Q. Cheng, S. Huo, Z. Liang, M. Fermeglia, S. Pricl, X. J. Liang, P. Rocchi and L. Peng, *Natl. Acad. Sci.*, 2015, **112**, 2978−2983.
25. H. Wang, J. Hu, X. Cai, J. Xiao and Y. Cheng, *Polym. Chem*., 2016, **7**, 2319−2322.
26. M. Marcos, R. Gimenez, J. L. Serrano, B. Donnio, B. Heinrich and D. Guillon, *Chem. Eur. J.,* 2001,**7**, 1006-1013.
27. Gaussian 16, Revision C.01, M. J. Frisch, G. W. Trucks, H. B. Schlegel, G. E. Scuseria, M. A. Robb, J. R. Cheeseman, G. Scalmani, V. Barone, G. A. Petersson, H. Nakatsuji, X. Li, M. Caricato, A. V. Marenich, J. Bloino, B. G. Janesko, R. Gomperts, B. Mennucci, H. P. Hratchian, J. V. Ortiz, A. F. Izmaylov, J. L. Sonnenberg, D. Williams-Young, F. Ding, F. Lipparini, F. Egidi, J. Goings, B. Peng, A. Petrone, T. Henderson, D. Ranasinghe, V. G. Zakrzewski, J. Gao, N. Rega, G. Zheng, W. Liang, M. Hada, M. Ehara, K. Toyota, R. Fukuda, J. Hasegawa, M. Ishida, T. Nakajima, Y. Honda, O. Kitao, H. Nakai, T. Vreven, K. Throssell, J. A. Montgomery, Jr., J. E. Peralta, F. Ogliaro, M. J. Bearpark, J. J. Heyd, E. N. Brothers, K. N. Kudin, V. N. Staroverov, T. A. Keith, R. Kobayashi, J. Normand, K. Raghavachari, A. P. Rendell, J. C. Burant, S. S. Iyengar, J. Tomasi, M. Cossi, J. M. Millam, M. Klene, C. Adamo, R. Cammi, J. W. Ochterski, R. L. Martin, K. Morokuma, O. Farkas, J. B. Foresman, and D. J. Fox, Gaussian, Inc., Wallingford CT, 2016.
28. S. Gürbüz, M. Idrisa and D. Tuncel *Org. Biomol. Chem.*, 2015, **13**, 330-347.
29. P. Sahoo, and P. Dastidar, *Cryst. Growth Des.* 2012, **12**, 5917-5924.
30. T. Lafitte, S. K Kumar and A. Z. Panagiotopoulos, *Soft Matter* 2014, **10**, 786-794.
31. L. Eberson, *J. Org. Chem.* 1962, **27**, 2329-2331.
32. N. L. Weinberg and H. R. Weinberg, *Chem. Rev.* 1968, **68**, 449-523.
33. A. Wiebe, T. Gieshoff, S. Mçhle, E. Rodrigo, M. Zirbes, and S. R. Waldvogel, *Angew. Chem. Int. Ed.* 2018, **57**, 5594 – 5619.
34. G. Pezzatini, H. Wei, and R. Guidelli, *Electroanalysis*, 1992 **4**, 129-132.
35. B. E. Conway, and M. Dzieciuch, *Canadian J. Chem.,* 1963, **41**, 21-37.
36. M. Garzoni, N. Cheval, A. Fahmi, A. Dananiand, and G. M. Pavan*, J. Am. Chem. Soc*., 2012, **134**, 3349−3357.
37. I. Bury, B. Heinrich. C. Bourgogne, D. Guillon, and B. Donnio, *Chem. A Eur. J.*, 2006, **12**, 8396-8413.
38. A. S. Ertürk, M. U. Gürbüz, and M. Tülü, *Marmara Pharmaceutical J.,* 2017, **21**, 385-399.
39. Y. Ji, X. Yang, and Y. Qian, *RSC Adv.,* 2014, **4**, 49535-49540.
40. E. Roeven, L. Scheres, M. M. J. Smulders, and H. Zuilhof, *ACS Omega,* 2019, **4**, 3000−3011.
41. L. Wang, J. Zhang, X. Guo, S. Chen, Y. Cui, Q. Yu, L. Yang, H. Sun, D. Gao, and D. Xie, *New J.Chem.,* 2018, **42**, 19740-19748.

